J Therm Anal Calorim (2009) 97:185–190
DOI 10.1007/s10973-009-0239-5

$SrSnO_3$:Nd obtained by the polymeric precursor method

Soraia Carvalho de Souza · Mary Cristina Ferreira Alves · A. Luiz M. de Oliveira · E. Longo · F. Ticiano Gomes Vieira · Rodinei Medeiros Gomes · L. E. B. Soledade · A. G. de Souza · Iêda M. Garcia dos Santos

ICTAC2008 Conference

Abstract In this work, the synthesis of Nd-doped $SrSnO_3$ by the polymeric precursor method, with calcination between 250 and 700 °C is reported. The powder precursors were characterized by TG/DTA and high temperature X-ray diffraction (HTXRD). After heat treatment, the material was characterized by XRD and infrared spectroscopy. Ester and carbonate amounts were strictly related to Nd-doping. According to XRD patterns, the orthorhombic perovskite was obtained at 700 °C for $SrSnO_3$ and $SrSn_{0.99}Nd_{0.01}O_3$. For $Sr_{0.99}Nd_{0.01}SnO_3$, the kinetics displayed an important hole in the crystallization process, as no peak was observed in HTXRD up to 700 °C, while a XRD patterns showed a crystalline material after calcination at 250 °C.

Keywords Perovskite · Stannate · Neodymium-doping · Thermal analysis by TG/DTA · HTXRD

Introduction

Perovskite structures have a simple crystalline structure, which includes different symmetries, with cubic, tetragonal or orthorhombic unit cells, besides these distorted cells [1, 2]. Stannates ($MSnO_3$, M = Ba, Sr, Ca) are important perovskite materials in ceramic technology, due to their wide applications as components of dielectric materials, thermally stable capacitors and humidity sensors [3, 4].

$SrSnO_3$ has an orthorhombic perovskite structure (Pbnm space group) with a high degree of pseudocubic symmetry at room temperature [3]. Distortion of this structure is due to the SnO_6 octahedra inclination and distortion [5], favoring a higher amount of electronic transitions in this material. Technological interest in $SrSnO_3$ is due to its optical, electric and magnetic properties, which lead to its application as condensers and, more recently, as humidity sensor.

Perovskites containing rare earth elements have been applied as electrodes [6, 7], luminescent materials and phosphors, especially in devices for artificial light production as cathode ray tube, lamps and radiography detectors [8]. These perovskites have become attractive in the last decade, due to the investigation of the energy migration process in electronic materials, leading to important electronic applications [9, 10]. Among them, ABO_3 (A = Ca, Ba and Sr; B = Ti, Zr, Si, Nb, Hf, etc.) activated with rare earth ions as Sm^{3+}, Tm^{3+}, Eu^{3+}, Pr^{3+}, Ce^{3+}, Tb^{3+}, Er^{3+} are promising candidates [11].

In this work, strontium stannate, $SrSnO_3$, was doped with neodymium, synthesized by the polymeric precursor method. The elimination of organic material and the perovskite crystallization were evaluated by thermal analysis techniques (TG/DTA and HTXRD). Infrared spectroscopy and X-ray diffraction were used to confirm these data.

A great advantage of the polymeric precursor method, in relation to other chemical synthesis methods, is its low cost, once the reagents used in larger amounts are relatively cheap, besides working at relatively low temperatures [12].

S. C. de Souza (✉) · M. C. F. Alves · A. L. M. de Oliveira · F. Ticiano Gomes Vieira · L. E. B. Soledade · A. G. de Souza · I. M. Garcia dos Santos
LACOM, Departamento de Química/CCEN, Universidade Federal da Paraíba, Campus I, João Pessoa, PB, Brazil
e-mail: soraia_cs@yahoo.com.br

E. Longo
CMDMC—LIEC, Instituto de Química, UNESP, Araraquara, SP, Brazil

R. M. Gomes
LSR, Departamento de Engenharia Mecânica/CT, UFPB, Campus I, João Pessoa, PB CEP 58059-900, Brazil

Experimental

In this work, $Sr_{1-x}Sn_{1-y}Nd_{x+y}O_3$, $x = 0.01$, was synthesized by the polymeric precursor method, whose details are already described in literature [12, 13]. The reagents used in the synthesis are presented in Table 1.

Carbon elimination was carried out by calcination in O_2 atmosphere at 250 °C for 24 h, after milling of the precursors in an attritor mill for 4 h in an alcoholic medium. The precursors were characterized by thermogravimetry (TG) and differential thermal analysis (DTA) in a SDT-2960, TA Instruments analyzer in air atmosphere with a flow rate of 110 mL/min and a heating rate of 10 °C/min up to 850 °C, with about 10 mg of sample weighted into alumina crucibles. Characterization was also done by high temperature X-ray diffraction (HTXRD). Measurements were carried out with Cu-$K\alpha$ radiation and nickel filter on a SIEMENS D5000 diffractometer equipped with an Edmund Buehler controllable high temperature thermostatic chamber. The heating unit consists of a vacuum heating chamber with a Pt heater, temperature controller to an accuracy of ±1 K and Pt–PtRh10% thermocouple to monitor the temperature of the sample during the measurements. The heating cycles were performed under ambient atmosphere at a constant heating rate of 40 K/min up to the soak temperature of 500, 600 and 700 °C. Once the temperature reached a constant value, the XRD patterns were collected using continuous scanning mode in the 2θ range 40–48° with a scanning speed of 0.02°/s at a counting time of 2.0 s per step. The total duration of XRD recording was 26.5 min.

After thermal treatment at 250, 300, 400, 500, 600 and 700 °C for 2 h, the material was characterized in relation to structural properties, using X-ray diffraction and infrared spectroscopy (IR). The XRD patterns were obtained using a D-5000 Siemens diffractometer, employing $K\alpha$ Cu radiation, using continuous scanning mode in the 2θ range of 20–70°, with a 0.02° step and a step time of 1.0 s. The IR analyses were performed using an MB-102 Bomem spectrophotometer, in the range from 4,000 to 400 cm^{-1}, using KBr pellets.

Results and discussion

Figure 1a, b show the TG and DTA curves of the $SrSnO_3$, $SrSn_{0.99}Nd_{0.01}O_3$ and $Sr_{0.99}Nd_{0.01}O_3$ precursors. The samples had three thermal decomposition steps, except for $SrSn_{0.99}Nd_{0.01}O_3$, which presented two steps. The first step was assigned to the elimination of water and gases adsorbed on the material surface with an endothermic peak in DTA curve at about 70 °C. The other steps were assigned to the combustion of the organic material leading to exothermic peaks. Mass loss associated to endothermic peaks above 720 °C was assigned to the carbonate decomposition. The thermal analysis data are presented in Table 2.

Table 1 Reagents utilized in the synthesis of $SrSnO_3$:Nd compounds

Reagent	Chemical Formula	Purity (%)	Supplier (location)
Tin chloride	$SnCl_2{\cdot}2H_2O$	99.9	J.T.Backer (México)
Strontium nitrate	$Sr(NO_3)_2$	99.0	Vetec (Brazil)
Neodymium oxide	Nd_2O_3	–	Merck (Germany)
Ammonium hydroxide	NH_4OH	P.A	Vetec (Brazil)
Nitric acid	HNO_3	65.0	Dinâmica (Brazil)
Citric acid	$C_6H_8O_7{\cdot}H_2O$	99.5	Cargill (Brazil)
Ethylene glycol	$HO{\cdot}CH_2{\cdot}CH_2{\cdot}OH$	99.0	Avocado (Brazil)

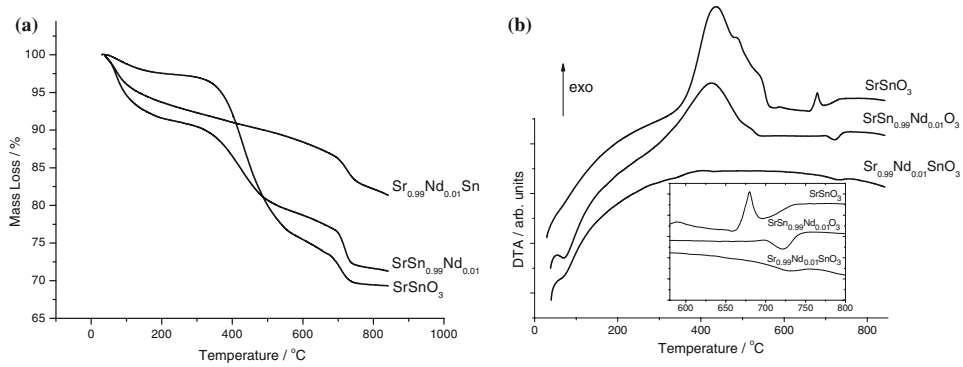

Fig. 1 TG (**a**) and DTA (**b**) curves of the $SrSnO_3$, $SrSn_{0.99}Nd_{0.01}O_3$ and $Sr_{0.99}Nd_{0.01}SnO_3$ powder precursors after heat treatment at 250 °C for 24 h in oxygen atmosphere

Table 2 Data from thermal analysis curves of the $SrSnO_3$, $SrSn_{0.99}Nd_{0.01}O_3$ and $Sr_{0.99}Nd_{0.01}SnO_3$ precursors

Sample	Steps	Temperature range (°C)	Mass loss (%)	DTA peak temperature (°C)
$SrSnO_3$	1	48–262	2.8	Not observed
	2	298–661	23.5	435, 489, 535 (exo)
	3	661–746	3.8	658 (endo), 680 (exo), 698 (endo)
$SrSn_{0.99}Nd_{0.01}O_3$	1	40–220	8.9	70 (endo)
	2	290–578	11.5	425 (exo)
	3	682–752	3.8	723 (endo)
$Sr_{0.99}Nd_{0.01}SnO_3$	1	40–100	5.5	70 (endo)
	2	100–687	6.8	–
	3	687–792	3.4	731 (endo)

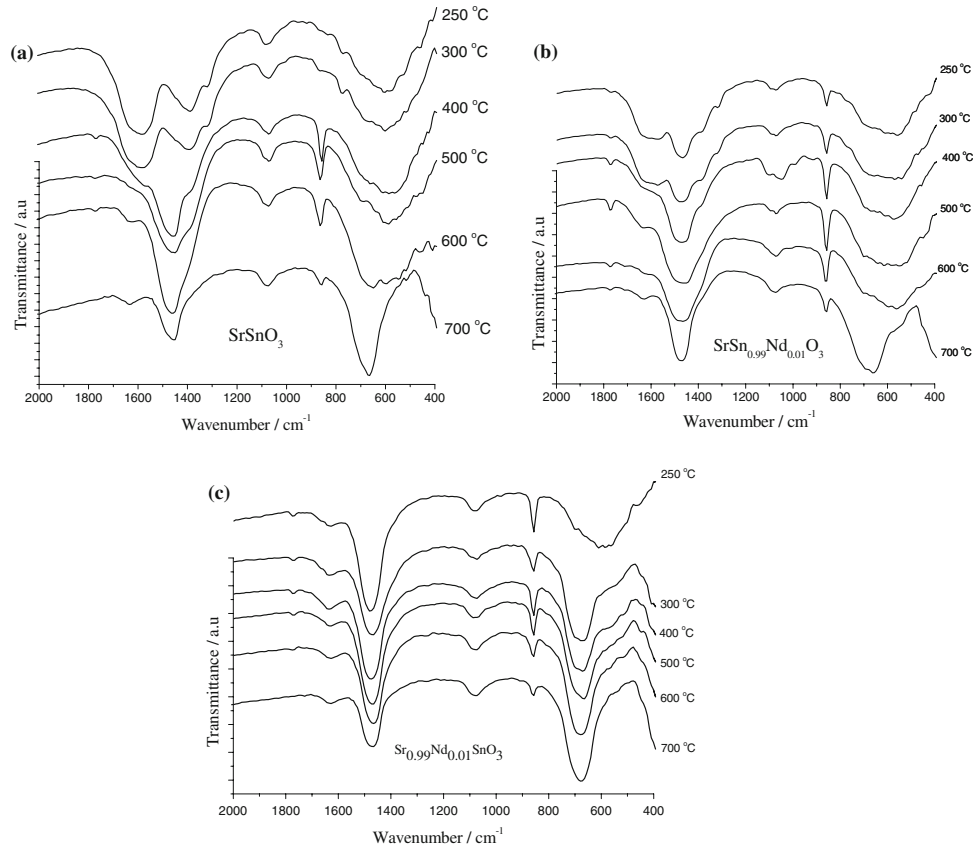

Fig. 2 IR spectra of $SrSnO_3$ (**a**), $SrSn_{0.99}Nd_{0.01}O_3$ (**b**) and $Sr_{0.99}Nd_{0.01}SnO_3$ (**c**), after calcination between 250 and 700 °C

The evaluation of the thermal decomposition steps was also done by infrared spectroscopy, after calcination at different temperatures (Fig. 2).

The IR spectra showed bands at 1,580–1,390 cm^{-1}, assigned to COO^- stretching in ester unidentate complexes [14, 15] and at 1,470, 1,080 and 862 cm^{-1} due to the presence of carbonates [14, 16, 17].

Ester bands were observed at low temperatures, decreasing in intensity with the temperature increase, disappearing after calcination at 600 °C. Comparing these results with TG/DTA data, the exothermic decomposition step may be assigned to ester combustion. For $Sr_{0.99}Nd_{0.01}SnO_3$, ester bands were not observed as well as the combustion peak in DTA curve.

In relation to carbonate bands, in $SrSnO_3$, its formation is only observed after calcination at 400 °C. With Nd-doping, its formation is already observed after calcination at 250 °C, independently of the substituted cation. A high amount of carbonate was observed at 500 and 600 °C, being eliminated at a higher temperature, according to TG/

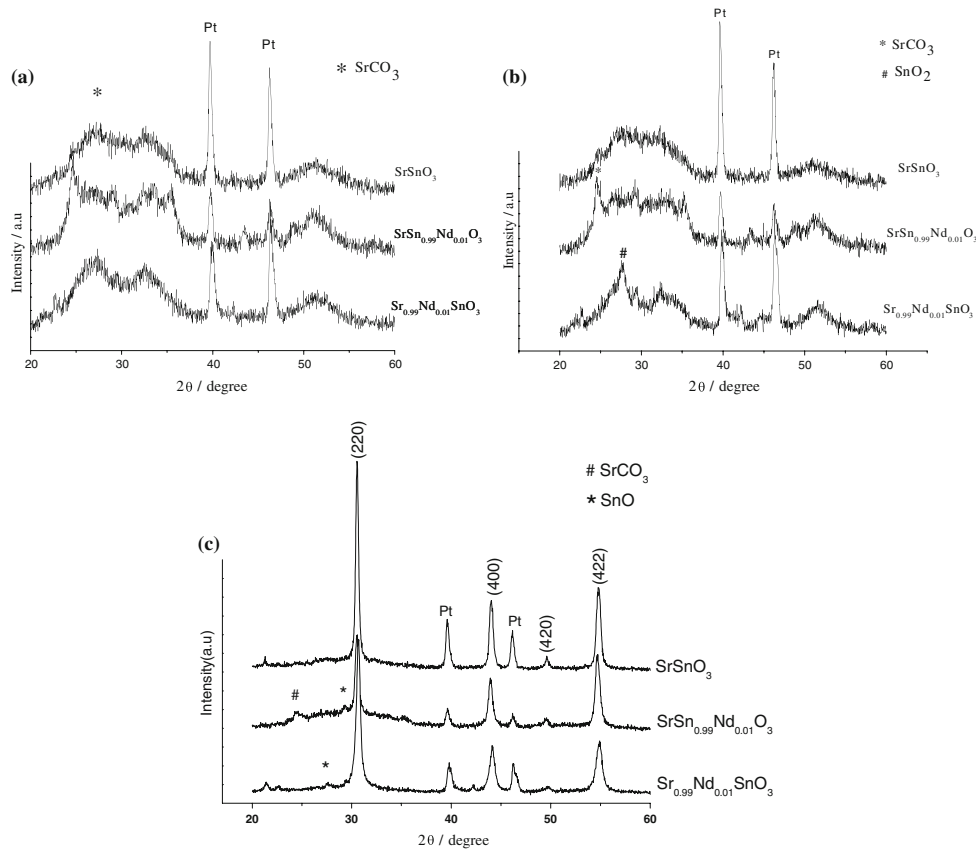

Fig. 3 HTXRD patterns of $SrSnO_3$, $SrSn_{0.99}Nd_{0.01}O_3$ and $Sr_{0.99}Nd_{0.01}SnO_3$ submitted to the temperatures of **a** 500 °C, **b** 600 °C and **c** 700 °C

DTA data. These bands are still observed after calcination at 700 °C, as the thermal stability is only achieved above 730 °C.

Bands assigned to the perovskite phase were detected after calcination at 700 °C, for pure $SrSnO_3$. A high short-range order was observed, as suggested by the high definition of the Me–O bands at 660 and below 500 cm^{-1} [17–19]. At 600 °C, the intensity of the band at 660 cm^{-1} already started to increase, but a low resolution is still observed.

When Nd replaced Sr (the lattice modifier), a higher definition of the Me–O band (around 600 cm^{-1}) was observed, even after calcination at 300 °C. This result indicated that this replacement led to a higher short-range order in the perovskite. The same behavior was not observed when Nd substituted Sn, which presented the same profile of the pure $SrSnO_3$, in relation to Me–O bands.

HTXRD patterns are presented in Fig. 3.

All samples were amorphous at 500 and 600 °C, with the perovskite crystallization noticed at 700 °C. In relation to secondary phases, different behaviors were observed, according to the Nd doping. Strontium carbonate was observed in the $SrSn_{0.99}Nd_{0.01}O_3$ in all temperatures, with decomposition above 700 °C. These results indicated that the endothermic peak at 731 °C in DTA curve was assigned to carbonate decomposition.

For $Sr_{0.99}Nd_{0.01}SnO_3$, SnO_2 precipitation occurs at 600 °C, indicating that Sr^{2+} may be also be replacing Sn^{4+} in the lattice.

Figure 4 shows the XRD patterns of the $SrSnO_3$ perovskites.

All diffraction peaks can be indexed as orthorhombic perovskite, with space group Pbnn, JCPDS file 77-1798. For pure $SrSnO_3$, crystallization occurred above 600 °C, with small peaks at this temperature and well-defined ones after calcination at 700 °C. These results were in agreement with the previous results, that showed an exothermic peak in DTA curve at 680 °C, besides an increase in short- and long-range order, according to IR spectra and HTXRD patterns.

For $SrSn_{0.99}Nd_{0.01}O_3$ (Fig. 4b), crystallization occurred at 700 °C, also in agreement with the IR spectra. For these samples, strontium carbonate was present in high amounts, and SnO precipitation occurred. This result may be assigned to Sn^{4+} reduction. This phase disappeared after calcination at 700 °C.

$Sr_{0.99}Nd_{0.01}SnO_3$ showed a different behavior. Well-defined peaks, assigned to perovskite, were already observed after calcination at 250 °C. This result was in agreement with the IR spectra, which already showed a high short-range order after calcination at this temperature. Comparison with HTXRD patterns showed that kinetic

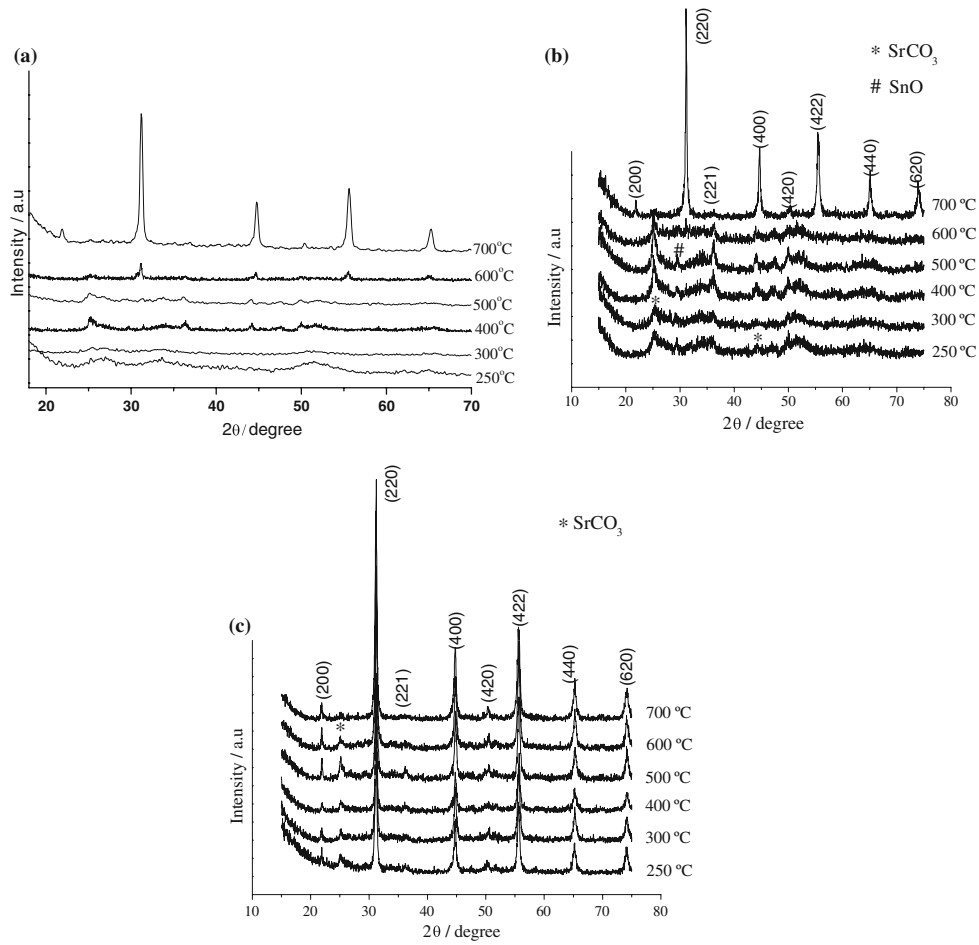

Fig. 4 X-ray diffraction patterns, after heat treatment at 250–700 °C, of **a** $SrSnO_3$, **b** $SrSn_{0.99}Nd_{0.01}O_3$ and **c** $Sr_{0.99}Nd_{0.01}SnO_3$

factor displayed an important hole in the perovskite crystallization, as HTXRD analysis was done under dynamic conditions, while IR spectra and XRD patterns were obtained after calcination at the indicated temperatures, for 2 h. For this sample, it may also be observed that the intensity of peaks assigned to strontium carbonate decreased after calcination at 700 °C.

Conclusions

Pure and Nd-doped Strontium stannates were synthesized by the polymeric precursor method. The precursor decomposition was evaluated. Exothermic peaks below 600 °C were assigned to the ester combustion. The amounts of esters and carbonates were strictly related to Nd-doping. Undoped samples only had carbonates above 400 °C. When Sn^{4+} was replaced by Nd^{3+}, carbonate was observed at 300 °C, besides esters. When Sr^{2+} was replaced, only carbonate was observed at 300 °C and no exothermic peak was observed in DTA. At 700 °C, the amount of carbonate decreased, in accordance to TG/DTA curves, which showed an endothermic peak related to carbonate decomposition. Analyses of XRD patterns revealed that $SrSnO_3$ with orthorhombic structure was obtained at 700 °C after calcination for 2 h for $SrSnO_3$ and $SrSn_{0.99}Nd_{0.01}O_3$. For $Sr_{0.99}Nd_{0.01}TiO_3$, higher short- and long-range orders were already observed after calcination at low temperature. Kinetics displays an important hole in crystallization process, as no peak was observed in HTXRD up to 700 °C, which was performed under dynamic conditions.

Acknowledgements The authors acknowledge CNPq/MCT, FINEP and CAPES for the financial support.

References

1. Pontes FM, Longo E, Leite ER, Lee EJH, Varela JA, Pizani PS, et al. Photoluminescence at room temperature in amorphous $SrTiO_3$ thin films obtained by chemical solution deposition. Mater Chem Phys. 2002;77:598–602.
2. Lu Z, Liu J, Tang Y, Li Y. Hydrothermal synthesis of $CaSnO_3$ cubes. Inorg Chem Commun. 2004;7:731–3.
3. Camargo ER. Síntese do $Pb(Mg_{1/3}Nb_{2/3})O_3$ (PMN) utilizando niobato de magnésio pelo método Pechini modificado, Universidade Federal de São Carlos. Brazil, MSc Thesis in Chemistry; 1998.

4. Udawatte CP, Kakihana M, Yoshimura M. Low temperature synthesis of pure $SrSnO_3$ and the $(Ba_xSr_{1-x})SnO_3$ solid solution by the polymerized complex method. Solid State Ion. 2000; 128:217–26.
5. Marinova Y, Hohemberger JM, Cordoncillo E, Escribano P, Carda JB. Study of solid solutions, with perovskite structure, for application in the field of the ceramic pigments. J Eur Ceram Soc. 2003;23:213–20.
6. Glerup M, Knight KS, Poulsen FW. High temperature structural phase transitions in $SrSnO_3$ perovskite. Mater Res Bull. 2005; 40:507–20.
7. Silva PRN. Emprego de óxidos tipo perovskita nas oxidações do propano e CO. Quím Nova. 2004;27:35–41.
8. Xiao XZ, Yan B. Matrix-induced synthesis and photoluminescence of M_2RENbO_6: Eu^{3+} (M = Ca, Sr, Ba; RE = Y, Gd, La) phosphors by hybrid precursors. J Alloy Compd. 2007;433:246–50.
9. Nieminen M, Sajavaara T, Rauhala E, Putkonen M, Niinistö L. Surface-controlled growth of $LaAlO_3$ thin films by atomic layer epitaxy. J Mater Chem. 2001;11:2340–5.
10. Nieminen M, Lehto S, Niinistö L. Atomic layer epitaxy growth of $LaGaO_3$ thin films. J Mater Chem. 2001;11:3148–53.
11. Lu Z, Chen L, Tang Y, Li Y. Preparation and luminescence properties of Eu^{3+}-doped $MSnO_3$ (M = Ca, Sr and Ba) perovskite materials. J Alloy Compd. 2005;387:L1–4.
12. Souza SC, Souza MAF, Lima SJG, Cassia-Santos MR, Fernandes VJ Jr, Soledade LEB, et al. The effects of Co, Ni and Mn on the thermal processing of Zn_2TiO_4. J Therm Anal Cal. 2005;79:455–9.
13. Alves MCF, Souza SC, Lima SJG, Longo E, Souza AG, Santos IMG. Influence of the precursor salts in the synthesis of $CaSnO_3$ by the polymeric precursor method. J Therm Anal Cal. 2007; 87:763–6.
14. Nakamoto K. Infrared and Raman spectra of inorganic and coordination compounds. New York: Wiley; 1980. p. 232.
15. Cho SG, Johnson PF, Condrate RA Sr. Thermal decomposition of (Sr, Ti) organic precursors during the Pechini process. J Mater Sci. 1990;25:4738–44.
16. Suasmoro S, Pratapa S, Hartanto D, Setyoko D, Dani UM. The characterization of mixed titanate $Ba_{1-x}Sr_xTiO_3$ phase formation from oxalate coprecipitated precursor. J Eur Ceram Soc. 2000; 20:309–14.
17. Nyquist RA, Kagel RO. Infrared spectra of inorganic compounds. San Diego: Academic Press Inc.; 1971. p. 78.
18. Licheron M, Jouarf G, Hussona E. Characterization of $BaSnO_3$ powder obtained by a modified sol-gel route. J Eur Ceram Soc. 1997;17:1453–7.
19. Vegas A, Vallet-Regý M, González-Calbet JM, Alario-Franco MA. The $ASnO_3$ (A=Ca,Sr) perovskites. Acta Cryst B. 1986;42: 167–72.